Tunable wetting properties of patterned silicon microchannels with varied surface free energy based on layer-by-layer nano self-assembly

J. Micromech. Microeng. **21** (2011) 045015 (8pp) doi:10.1088/0960-1317/21/4/045015

Tunable wetting properties of patterned silicon microchannels with varied surface free energy based on layer-by-layer nano self-assembly

Tao Zhang and Tianhong Cui[1]

Department of Mechanical Engineering, University of Minnesota, Minneapolis, MN 55455, USA

E-mail: tcui@me.umn.edu

Received 30 December 2010, in final form 4 February 2011
Published 10 March 2011
Online at stacks.iop.org/JMM/21/045015

Abstract

The wetting properties of patterned silicon microchannels with tunable surface free energy through coating hydrophilic TiO_2 nanoparticles using the layer-by-layer nano self-assembly technique is presented in this paper. The wettability of microchannels is tested by measuring the contact angle of a water droplet on the substrate. The capillary rise rate is tested by measuring the front location of a liquid on the silicon microchannel surface laid on a 45° inclined platform. It is found that the silicon microchannels with tunable surface free energy have super-hydrophilic wettability, and demonstrate a powerful capillary. For the silicon microchannels 200 μm wide, the liquid front can move up 40 mm in approximately 3 s. Fourier transformed infrared spectroscopy and x-ray photoelectron spectroscopy reveal the generation of –OH radicals after coating TiO_2 nanoparticles, verifying that the –OH radicals have a strong effect on the hydrophilicity. The patterned super-hydrophilic microchannels provide potential applications to microfluidic systems and heat diffusion systems based on tunable surface energy.

(Some figures in this article are in colour only in the electronic version)

1. Introduction

The microfluidic channel is one of the major features in microfluidic devices. Manipulating liquid, water in particular inside the microchannel, is very crucial in the design and fabrication of microfluidic devices for applications to biological sensing, diagnostic testing, and two-phase electronics cooling systems [1, 2]. Wetting properties have significant effects on liquid behavior in microfluidic systems [3], for example, a surface effect is the basis of capillary pumping [4], and light-driven motion of liquids on a photoresponsive substrate [5]. Well-controlled surface free energy along the microchannel walls can be tuned to promote the wetting properties of microchannel surfaces.

Many surface free energy patterning methods have been developed to achieve hydrophilic or hydrophobic microchannels. Plasma or UV treatment is the most common method for patterning surface free energy in microfluidic systems [6]. Plasma or UV modification processes generate new chemical properties on the polymer surface due to chemical reaction and physical reaction between surfaces and active gas species. Many different types of gas plasma reported, such as air, oxygen, UV-ozone, H_2O and ammonia, modify the polymer surface. UV polymer grafting is one of the techniques to pattern surface free energy in microfluidic devices, similar to the plasma technique [7]. Different monomers such as acrylic acid, acrylamide, dimethylacrylamide (DMA), 2-hydroxyethyl acrylate, and PEG-monomethoxyl acrylate were grafted onto polymer surfaces to increase hydrophilic properties. One straightforward method to pattern surface free energy is the self-assembly of the polymer monolayer or multilayer [8]. Monolayer surface modification is

[1] Author to whom any correspondence should be addressed.

obtained by coating the solution or gas stream within microchannels. Multilayer surface modification is obtained by coating with alternating layers of positively and negatively charged polyelectrolytes on any charged surface. Zhao *et al* [9] indicated that a self-assembled monolayer was used in combination with either multi-stream laminar flow or photolithography to pattern surface energies inside microchannel networks. Another method is to deposit hydrophilic or hydrophobic oxide on a substrate. Jung *et al* [10] deposited a hydrophilic titanium dioxide film using a sol–gel process. Nakamura *et al* [11] prepared hydrophilic SiO_2/TiO_2 bi-layer films using vacuum evaporation. Koshizakii *et al* [12, 13] fabricated a super-hydrophilic TiO_2 nanocolumn array by pulsed laser deposition (PLD) using a polystyrene (PS) colloidal monolayer as a template under a high pressure (6.7 Pa) of background oxygen gas.

The above methods are used as traditional methods of surface free energy patterning in microfluidic systems. However, there are some disadvantages such as requirement for special instruments, harsh processing conditions, high cost, etc. The layer-by-layer (LbL) self-assembly technique offers an easy and inexpensive process for multilayer formation, allowing a variety of materials to be incorporated within a film structure. This technique can be performed at room temperature, and beakers and tweezers are the only apparatus required. The LbL technique has been investigated since last century by our group [14, 15].

In this paper, an effective approach with surface free energy through coating hydrophilic TiO_2 nanoparticles using LbL nano self-assembly is presented. In our experiment, the hydrophilic films are built with alternating layers of negatively charged PSS and positively charged TiO_2. Before the TiO_2 nanoparticle coating, some polyion PDDA/PSS films were coated to enhance the adsorption of TiO_2 nanoparticles. The patterned silicon microchannels are coated with LbL TiO_2 nanoparticles at room temperature, demonstrating various wetting properties with the TiO_2 layers. Silicon microchannels have a super-hydrophilic property and a powerful capillary after four layers of TiO_2 nanoparticle deposition. For microchannels 200 μm wide, the contact angle is zero, and the liquid front can move up 40 mm in approximately 3 s. The wetting properties are verified by Fourier transform infrared spectroscopy (FTIR) and x-ray photoelectron spectroscopy (XPS) analysis.

2. Experimental details

2.1. LbL nano self-assembly

LbL self-assembly is mainly conducted through electrostatic interaction. Alternation of the surface charges results in a continuous assembly between positively and negatively charged materials with a great freedom in layers and deposition sequence [16]. In our experiment, the polyions involved in the fabrication process are positively charged poly(dimethyldiallyl-ammonium chloride) (PDDA) and negatively charged poly(styrenesulfonate) (PSS). These

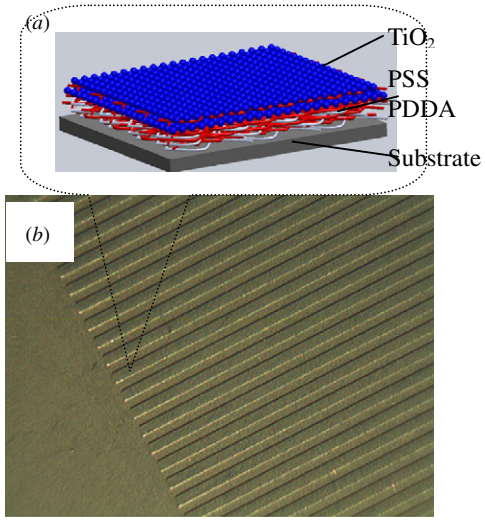

Figure 1. (*a*) Schematic illustration of layer-by-layer self-assembly of TiO_2 nanoparticles, and (*b*) image of patterned silicon microchannels.

polyion films (PDDA/PSS) enhance the adsorption of subsequent nanoparticles. The reliability of the TiO_2 hydrophilic film will be enhanced [17]. The concentrations of PDDA and PSS are 80 and 20 mg mL^{-1}, respectively. Both solutions were mixed with 0.5 M NaCl to increase their ionized strength. TiO_2 nanoparticles less than 75 nm in diameter are used as the hydrophilic material. The concentration of the TiO_2 nanoparticle solution is 20 mg mL^{-1}. All the above materials were purchased from Sigma-Aldrich Corporation.

Silicon microchannels are fabricated by photolithography and inductive coupling plasma (ICP) dry etching (figure 1(*b*)); the dimensions of the microchannels are 40 mm long, 200 μm wide and 100 μm deep. The space between two microchannels is 200 μm. As shown in figure 1(*a*), the substrates were alternately immersed in aqueous PDDA and PSS solutions, in a sequence of [PDDA (10 min) + PSS (10 min)]$_2$. The subscript 2 designates the number of immersions. The two bi-layers of PDDA/PSS served as precursor layers to enhance the subsequent adsorption of conjugated polymers and nanoparticles. Between two immersions of the substrate into solutions, there was an intermediate rinsing using DI water for 1 min to remove residues on the previous layer. Following the precursor layers, four layers of TiO_2 nanoparticles were coated on the substrate surface in the sequence of [TiO_2 (10 min) + PSS (10 min)]$_4$.

2.2. Contact angle measurements

Contact angles of water drops were measured with a contact angle meter (DATAPHYSICS, OCA15 Plus). To get statistically sound results, we typically measured at least five droplets for each sample. The representative contact angle was taken as the mean of these different determinations, and the corresponding error was estimated to be typically $\pm$ 20%.

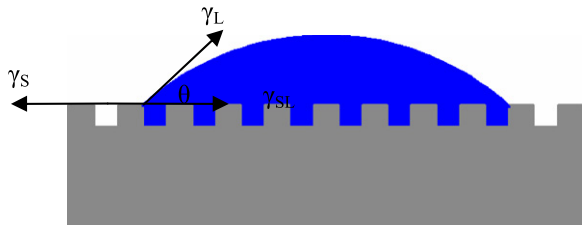

Figure 2. Schematics of the contact angle measurement.

2.3. Surface free energy

The calculation of the surface free energy of silicon microchannels is performed in the SE calculation window of the contact angle meter. The equation of state theory method is chosen to calculate the surface free energy. This is the method used for any universal system (polymers, aluminum, coatings, varnishes). This method requires at least one testing fluid for the contact angle determination. In this paper, DI water, acetone and methanol are used as testing liquids during the calculation of surface free energy.

2.4. Capillary rise rate testing

A simple capillary rise rate testing system including a 45° inclined platform, glass reservoir and camera is set up to record the changing interface of liquid–air in silicon microchannels (figure 5(*a*)). The base of the inclined platform rests in a reservoir filled gradually with water. When liquid reaches the bottom edge of the silicon microchannel surface, water climbs the inclined wafer. A video camera records the moving front of this water as it rises from the base of the mesh to the top edge. The MATLAB image processing code is used to analyze the video and determine the capillary rise rate by tracking the location of the water front at each frame.

2.5. FTIR, XPS and SEM characterization

The TiO_2 films are characterized by FTIR transmission spectroscopy in a range of 4000–500 cm^{-1} with a resolution of 4 cm^{-1} using a Nicolet Series II Magna-IR System 750 spectrometer. Spectra corresponding to 100 scans are recorded in room atmosphere after purging the measurement chamber with dry air for 10 min. Surface analysis is performed by XPS from vacuum employing a Mg K_α source (1253.6 eV). The x-ray source is operated at 20 kV at a current of 80 mA. A scanning electron microscope (JEOL 6500) is used to take SEM images of microstructures and TiO_2 nanoparticles.

3. Results and discussion

3.1. Contact angle testing and surface free energy of patterned silicon microchannels

The contact angle is the angle between a solid surface and a liquid where a free surface of static droplet contacts a solid surface, as a result of wettability. The theory of the contact angle of pure liquids on a solid was developed as the Young equation [18]

$$\gamma_L \cos\theta = \gamma_S - \gamma_{SL}. \quad (1)$$

Figure 2 is the schematic representation of the contact angle measurement for the patterned silicon microchannels. γ_L is the experimentally determined surface tension of the liquid–vapor, working as a force to spread liquid once attached to a solid surface. γ_S is the surface free energy of the solid–vapor interface, working as a force to minimize the surface area of the liquid itself. γ_{SL} is the solid–liquid interfacial energy, as a force that does not contribute to the work of spreading. θ is the contact angle determined by the balance of γ_L, γ_S and γ_{SL}.

In this paper, the wettability of silicon microchannels is studied in ambient air at room temperature using a contact angle meter based on the sessile drop method. The mean contact angles are determined by averaging values measured at five different points on the sample surface.

Wettability is tested by measuring the contact angle of a water droplet on a substrate. Figure 3 shows the contact angle images of patterned silicon microchannels. Figure 3(*a*) shows the contact angle of a water drop (5 μL) on an etched silicon microchannel, and the contact angle is 160°. As shown in figures 3(*b*) and (*c*), the contact angle is 86° after coating one layer of PDDA/PSS and 45° after coating two layers of PDDA/PSS. As shown in figures 3(*c*)–(*e*), it is found that water completely wetted the silicon microchannel surface with a contact angle of 0° after coating three layers of TiO_2 nanoparticles, while the contact angle is about 21° and 13° after coating one and two layers of TiO_2, respectively. This dramatic drop in contact angles indicates that the silicon microchannel surface becomes super-hydrophilic with more TiO_2 nanoparticles.

Figure 4 shows the contact angle of smooth silicon and etched silicon without microchannels coated by different layers of TiO_2 particles. It is found that the contact angle decreases with increasing layers. The contact angle is 8° after coating four layers of TiO_2 nanoparticles.

As for the etched silicon, the roughness is 13.7 nm after etching by ICP. However, the roughness is 15.2, 22.6, 37.3 and 43.6 nm, respectively, when the etched silicon is coated with one, two, three or four layers of TiO_2 particles. It is found that the contact angle decreases with increasing layers. In fact, for the silicon wafer (smooth or etched) without the microchannel, there is no liquid diffusion on the silicon surface and no capillary phenomenon, even coating four or more layers of TiO_2 nanoparticles. It is possible that both the surface structures (primary structure) and the intermolecular interactions (secondary structure) have critical contributions to the capillary effect. However, the primary structure has a stronger contribution than the secondary structure based on the experiments in this paper.

It agrees with the measurement of the contact angle on a given solid surface, the most practical way to obtain the surface energy [19]. To obtain the solid surface free energy, γ_S, an estimate of γ_{SL} has to be obtained. Among the various possible

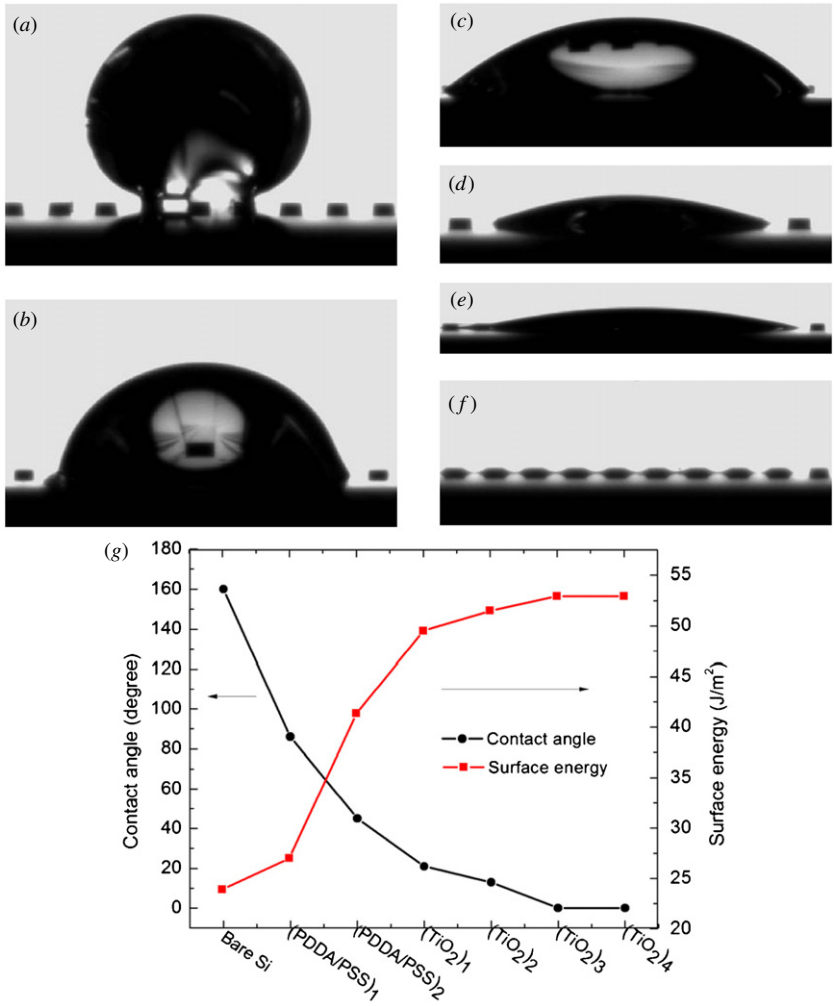

Figure 3. Contact angle images of patterned silicon microchannels: (*a*) etched silicon microchannels; (*b*) after coating one bi-layer of PDDA/PSS; (*c*) after coating two bi-layers of PDDA/PSS; (*d*) after coating one layer of TiO_2 nanoparticles; (*e*) after coating two layers of TiO_2 nanoparticles; (*f*) after coating three layers of TiO_2 nanoparticles; and (*g*) variation of the contact angle and surface free energy with the coating process.

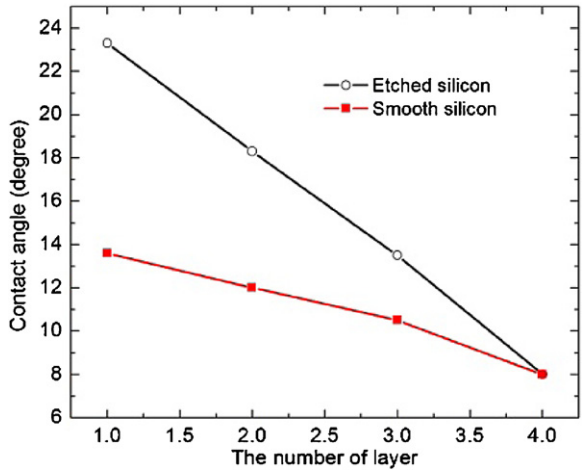

Figure 4. Variation of the contact angle of smooth silicon and etched silicon without microchannels coated by different layers of TiO_2 particles.

approaches to determine γ_S and γ_{SL}, the state approach has been selected. Neumann *et al* [20] and Li *et al* [21] derived an equation of state for the solid–liquid interfacial surface energy:

$$\gamma_{SL} = \gamma_S + \gamma_L - 2\sqrt{\gamma_S \gamma_L}\, e^{-\beta(\gamma_L - \gamma_S)^2}. \quad (2)$$

Combining this equation with the Young equation (1), the following equation is obtained:

$$\gamma_L(1 + \cos\theta) = 2\sqrt{\gamma_S \gamma_L}\, e^{-\beta(\gamma_L - \gamma_S)^2} \quad (3)$$

where $\beta = 0.000\,1247$ (m mN $^{-1})^2$ was obtained by fitting equation (3) to accurate contact angle data on polymeric solids. Kwok and Neumann [22] modified equation (2), and derived an equation of state for the solid–liquid interfacial surface energy:

$$\gamma_{SL} = \gamma_S + \gamma_L - 2\sqrt{\gamma_S \gamma_L}[1 - \beta_1(\gamma_S - \gamma_L)^2]. \quad (4)$$

In conjunction with the Young equation (1), the current form of the state equation is given by

$$\gamma_L(1 + \cos\theta) = 2\sqrt{\gamma_S \gamma_L}[1 - \beta_1(\gamma_S - \gamma_L)^2] \quad (5)$$

where β_1 is 0.000 1057 (m mN$^{-1})^2$. Equations (3) and (5) enable the evaluation of the surface free energy of a solid γ_S from a single contact angle measurement of a liquid with a

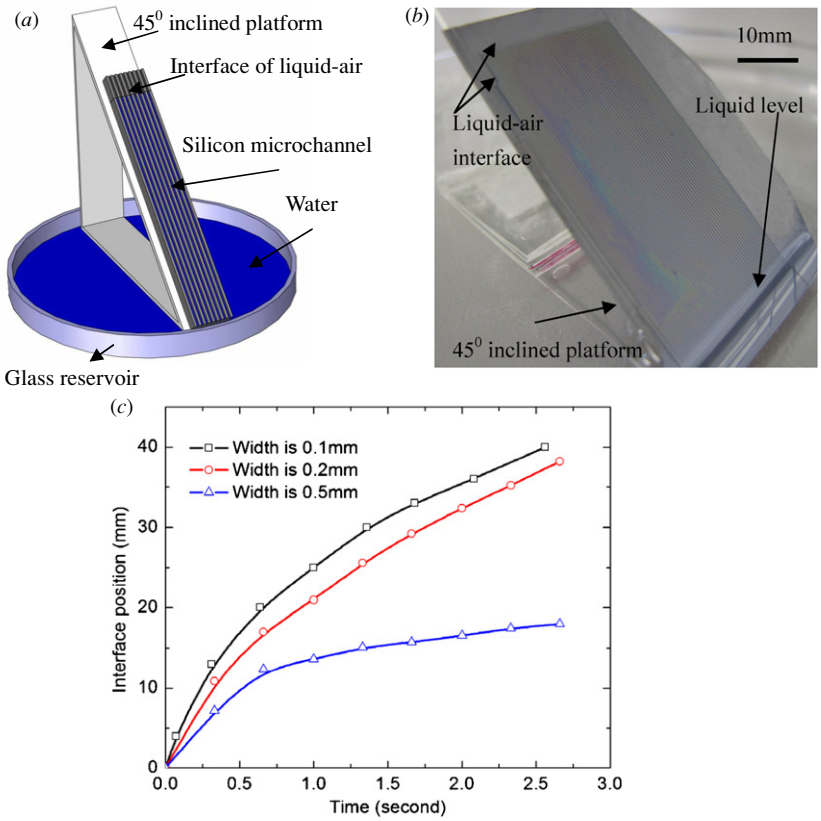

Figure 5. (*a*) Schematic diagram of the capillary rise rate testing system. (*b*) The testing platform for the capillary rise rate. (*c*) Capillary rise rate versus time with different silicon microchannels.

Table 1. Testing data of the contact angle for three liquids and the calculation results of free surface energy.

	Contact angle (°)			
	DI water	Acetone	Methanol	Surface energy (J m^{-2})
Bare silicon	160	0	0	23.9
$(PDDA/PSS)_1$	86	0	0	27
$(PDDA/PSS)_2$	45	0	0	41.33
$(TiO_2)_1$	21	0	0	49.5
$(TiO_2)_2$	13	0	0	51.5
$(TiO_2)_3$	0	0	0	52.94

The subscripts 1, 2 and 3 outside bracket designate the layer number.

known surface tension, γ_L. However, neither the dispersion nor the polar component can be evaluated.

To achieve meaningful results for the surface free energy of silicon microchannels, three liquids were used. In this paper, DI water, acetone and methanol are used as testing liquids during the calculation of surface free energy. Table 1 shows the testing data of contact angles for the three liquids and the calculation results of surface free energy by the contact angle meter. Figure 3(*g*) shows the variation of contact angles and surface free energy with the coating process. It is found that the surface free energy is only 23.9 J m^{-2} for the bare silicon microchannels, and it increases with the coating of PDDA/PSS and TiO_2 nanoparticles. After coating three layers of TiO_2 nanoparticles, the curve of surface free energy is saturated.

3.2. Capillary rise rate testing

Wetting and its associated surface forces are responsible for other relevant phenomena, including capillary effects. This implies that the capillary rate and capillary pressure are important parameters indicating wettability. The Young–Laplace equation asserts that the capillary pressure is directly proportional to the height of a water front location because a greater capillary pressure forces liquid to rise higher on the substrate, and the capillary rise rate can be used qualitatively to denote the capillary pressure [23]. We can characterize the capillary rise rate by noting the changing location of the water front in the silicon microchannels at each instant. As shown in figure 5(*b*), the patterned silicon microchannels are set on a test platform inclined at 45°. The base of the inclined platform rests in a reservoir filled gradually with DI water. When liquid reaches the bottom edge of the silicon microchannel, water climbs the inclined microchannel. A video camera can be used to record the moving front of water as it rises from the base of the silicon microchannels, and the video is exported to a computer. The MATLAB image processing code is used to analyze the video, and determine the capillary rise rate by tracking the location of water front in microchannels at each frame. In order to record the interface of liquid–air in microchannels clearly, a batch of parallel microchannels is patterned on the silicon wafer surface. Figure 5(*c*) shows the variation of the capillary rise rate with different silicon microchannels. It is found that for the microchannels 200 μm wide, the liquid front can move up 40 mm in approximately

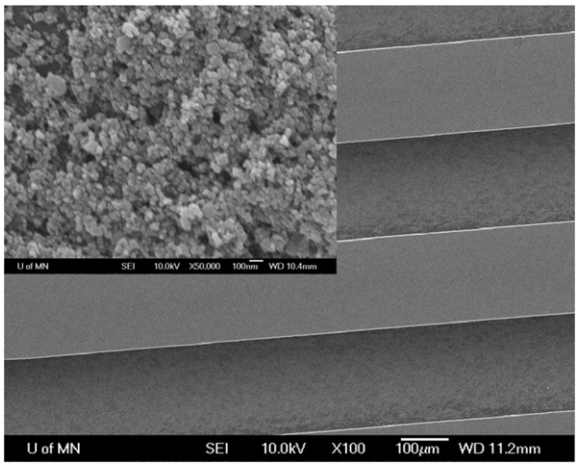

Figure 6. SEM image of silicon microchannels after coating TiO_2.

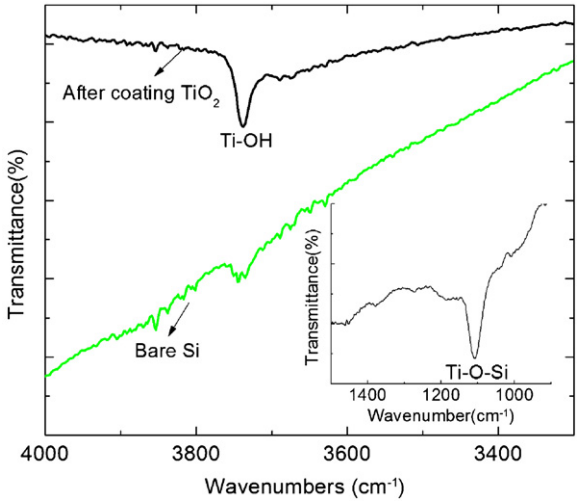

Figure 7. FTIR spectra in the hydroxyl region of the TiO_2 film.

3 s. On the other hand, the capillary rise rate decreases with increasing width of microchannels. For the channel 500 μm wide, the liquid front can move up approximately 20 mm. However, for the same silicon microchannels, there is no water diffusion and capillary rise phenomenon before the TiO_2 nanoparticles coating.

3.3. Characterization of SEM, FTIR, and XPS

Figure 6 shows the SEM image of silicon microchannels coated with TiO_2 nanoparticles. Some composite microstructures can be observed from the image inset in figure 6, contributing to the capillary action inside the microchannels.

Because the –OH groups have a strong effect on the film hydrophilicity [24], we investigate the silicon surfaces with coatings using FTIR and XPS to explain the reason for the high capillary rise rate inside the silicon microchannels after coating TiO_2 nanoparticles. However, water can affect the final interpretation of –OH absorption bonds. Therefore to minimize water adsorption, the measurement chamber was purged with dry air for 10 min before collecting the FTIR

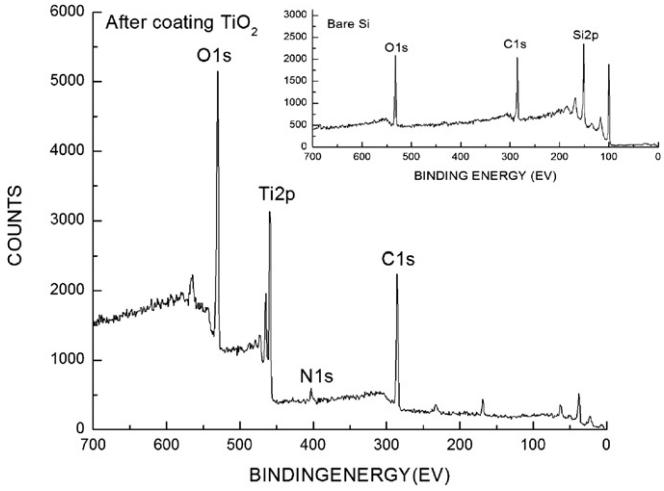

Figure 8. Wide XPS spectra of an etched Si (1 0 0) wafer, compared to the same substrate after functionalization with TiO_2 nanoparticles.

data. FTIR absorption spectra in the hydroxyl region (3800–3200 cm^{-1}) are illustrated in figure 7. A sharp absorption peak is located at about 3745 cm^{-1}, corresponding to the isolated surface –OH groups. However, for the freshly etched bare silicon, a weaker peak is found at the same location. It is also indicated from the low wave number region between 1400 and 900 cm^{-1}, in the inset of figure 7. The film spectra exhibit the typical absorption bonds of Ti–O–Si at about 1075 cm^{-1} [25].

XPS is a suitable method traditionally used to study surface chemical properties, which can provide insights into surface mechanisms yielding a natural super-hydrophilicity. In this paper, XPS is used to investigate the surface chemical state of the freshly deposited TiO_2 film; the film is studied within the first 12 h following the deposition. Figure 8 shows the wide scanned XPS spectra (survey) of a freshly etched Si (1 0 0) wafer, as compared to the same substrate after functionalization with TiO_2 nanoparticles. It is found from the inset spectra in figure 8 that no further components are observed on the high energy side of the peak, where the presence of silicon oxides would be expected. These findings indicate that no oxidation of the silicon surface has occurred during the etching procedure or immediately before the grafting process. Besides the Si 2p region, weak signals due to C 1s (∼285 eV) and O 1s (∼532 eV) lines are also detected on the freshly etched bare silicon microchannel, and they are attributed to adventitious contaminants that cannot be completely removed during etching and handling steps. Analysis of the composition for the etched bare silicon surface revealed carbon and oxygen at 34% and 13%, respectively. After coating TiO_2 nanoparticles, the XPS survey scan spectrum (figure 8) shows variations, mainly due to the increase of C 1s and O 1s peaks and the appearance of the Ti 2p peak.

Because the hydrophilic properties of TiO_2 film surfaces rely on the presence of surface OH groups, the peaks located at 532 and 530 eV were investigated. Basically, the O 1s peak could be decomposed into two components, one at about 530 eV is assigned as bulk oxide (O^{2-}) and the peak at about 532 eV is assigned as hydroxyl (OH) species. Figure 9 is

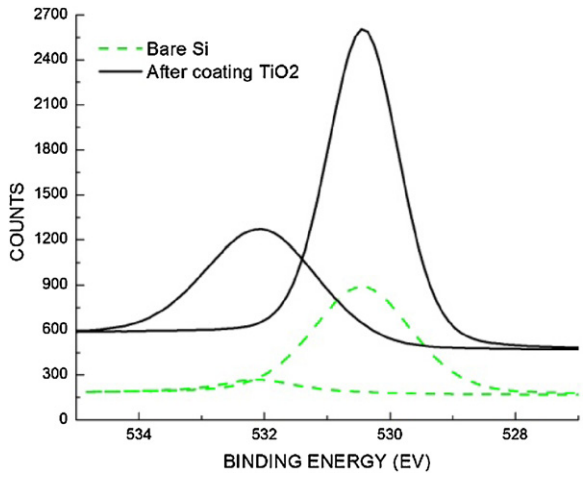

Figure 9. High-resolution XPS spectra of O 1s.

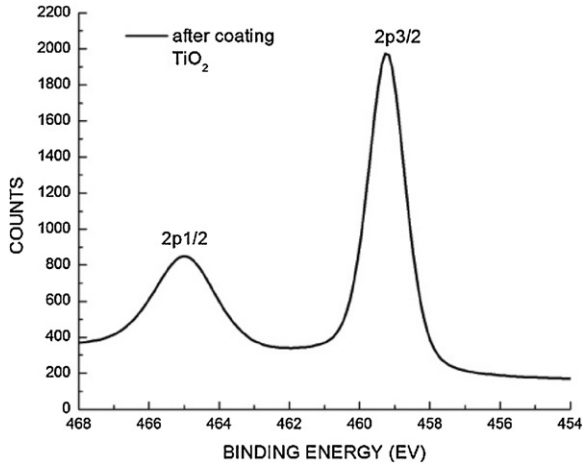

Figure 10. High-resolution XPS spectra of Ti 2p.

the high-resolution XPS spectra of O 1s of the TiO_2 film and bare silicon. It can be seen that the O 1s BE is observed at 530.45 eV due to the O^{2-} group and at 531.05 eV due to the OH group. When the sample was coated with TiO_2, it had higher OH binding energy than before the coating (bare silicon). The locations of the binding energy for these peaks agree with the reported values for the bulk oxide and hydroxyl species [26].

Figure 10 shows the high-resolution XPS spectra of Ti 2p. It is found that the Ti 2p1/2 and Ti 2p3/2 spin-orbital splitting photoelectrons are located at binding energies of 464.95 and 459.22 eV, respectively. The peak separation of 5.73 eV between the Ti 2p1/2 and Ti 2p3/2 signals is in excellent agreement with the one reported in the handbook of x-ray photoelectron spectroscopy [27].

4. Conclusions

The wettability of patterned silicon microchannels with varied surface free energy through coating hydrophilic TiO_2 nanoparticles using the layer-by-layer nano self-assembly technique is presented in this paper. Layer-by-layer nano self-assembly together with photolithography is very effective to pattern surface free energy. A tunable surface free energy can be achieved by coating different layers of TiO_2 nanoparticles. The silicon microchannels patterned surface free energy with TiO_2 nanoparticles coatings by self-assembly has super-hydrophilic wettability, and demonstrates a powerful capillary effect. For the silicon microchannels 200 μm wide, the liquid front can move up 40 mm in approximately 3 s. FTIR and XPS reveal the generation of –OH radicals after coating TiO_2 nanoparticles, verifying that the –OH radicals have a strong effect on the hydrophilicity. The patterned super-hydrophilic microchannels provide potential applications to surface tension driven microfluidic systems and heat diffusion systems.

Acknowledgment

We are grateful to the Nanofabrication Center and the Characterization Facility at the University of Minnesota for their assistance with fabrication and characterization.

References

[1] Gallardo B S *et al* 1999 Electrochemical principles for active control of liquids on submillimeter scales *Science* **283** 57–60
[2] Berthier E and Beebe D J 2007 Flow rate analysis of a surface tension driven passive micropump *Lab Chip* **7** 1475–8
[3] Handique K, Gogoi B P, Burke D T, Mastrangleo C H and Burns M A 1997 Microfluidic flow control using selective hydrophobic patterning *Proc. SPIE* **3224** 185–95
[4] Delamarche E, Bernard A, Schmid H, Michel B and Biebuyck H 1997 Patterned delivery of immunoglobulins to surfaces using microfluidic networks *Science* **276** 779–81
[5] Ichimura K, Oh S K and Nakagawa M 2000 Light-driven motion of liquids on a photoresponsive surface *Science* **288** 1624–6
[6] Zhou J, Ellis A V and Voelcker N H 2010 Recent developments in PDMS surface modification for microfluidic devices *Electrophoresis* **31** 2–16
[7] Hu S, Ren X, Bachman M, Sims C E, Li G P and Allbritton N 2002 Surface modification of poly(dimethylsiloxane) microfluidic devices by ultraviolet polymer grafting *Anal. Chem.* **74** 4117–23
[8] Kumlangdudsana P, Dubas S T and Dubas L 2007 Surface modification of microfluidic devies *J. Met. Mater. Miner.* **17** 67–74
[9] Zhao B, Moore J S and Beebe D J 2001 Surface-directed liquid flow inside microchannels *Science* **291** 1023–6
[10] Jung C-K, Bae I-S, Song Y-H, Kim T-K, Vlcek J, Musil J and Boo J-H 2005 Synthesis of TiO_2 photocatalyst and study on their improvement technology of photocatalytic activity *Surf. Coat. Technol.* **200** 534–8
[11] Nakamura M, Kobayashi M, Kuzuya N, Komatsu T and Mochizuka T 2006 Hydrophilic property of SiO_2/TiO_2 double layers film *Thin Solid Films* **502** 121–4
[12] Li Y, Sasaki T, Shimizu Y and Koshizaki N 2008 A hierarchically ordered TiO_2 hemispherical particle array with hexagonal-non-close-packed tops: synthesis and stable superhydrophilicity without UV irradiation *Small* **4** 2286–91
[13] Li Y, Sasaki T, Shimizu Y and Koshizaki N 2008 Hexagonal-close-packed, hierarchical amorphous TiO_2 nanocolumn arrays: transferability, enhanced photocatalytic activity, and superamphiphilicity without UV irradiation *J. Am. Chem. Soc.* **130** 14755–62

[14] Xue W and Cui T 2007 Characterization of layer-by-layer self-assembled carbon nanotube multilayer thin films *Nanotechnology* **18** 1–7

[15] McDonald B T and Cui T 2011 Superhydrophilic surface modification of copper surfaces by layer-by-layer self-assembly and liquid phase deposition of TiO_2 thin film *J. Colloid Interface Sci.* **354** 1–6

[16] Cui T, Hua F and Lvov Y 2004 FET fabricated by layer-by-layer nano assembly *Papers Transducers'04 Conf. (March)* pp 503–6

[17] Ariga K, Hill J P and Ji Q M 2007 Layer-by-layer assembly as a versatile bottom-up nanofabrication technique for exploratory research and realistic application *Phys. Chem. Chem. Phys.* **9** 2297–436

[18] Leroy F and Plathe F M 2011 Rationalization of the behavior of solid–liquid surface free energy of water in Cassie and Wenzel wetting states on rugged solid surfaces at the nanometer scale *Langmuir* **27** 637–45

[19] Wu W and Nancollas G H 1999 Determination of interfacial tension from crystallization and dissolution data: a comparison with other methods *Adv. Colloid Interface Sci.* **79** 229–79

[20] Neumann A W, Good R J, Hoppe C J and Sejpal M 1974 An equation-of-state approach to determine surface tensions of low-energy solids from contact angles *J. Colloid Interface Sci.* **49** 291–304

[21] Li D and Neumann A W 1992 Contact angles on hydrophobic solid surfaces and their interpretation *J. Colloid Interface Sci.* **148** 190–200

[22] Kwok D Y and Neumann A W 2000 Contact angle interpretation in terms of solid surface tension *Colloids Surf.* A **161** 31–48

[23] Chan W K and Yang C 2005 Surface-tension-driven liquid–liquid displacement in a capillary *J. Micromech. Microeng.* **15** 1722–8

[24] Nakamura M, Sirghi L, Aoki T and Hatanaka Y 2002 Study on hydrophilic property of hydro-oxygenated amorphous TiO_x:OH thin films *Surf. Sci.* **507–510** 778–82

[25] Permpoon S, Houmard M, Riassetto D, Rapenne L, Berthome G, Baroux B, Joud J C and Langlet M 2008 Natural and persistent superhydrophilicity of SiO_2/TiO_2 and TiO_2/SiO_2 bi-layer films *Thin Solid Films* **516** 957–66

[26] Erdem B, Hunsicker R A, Simmons G W, Sudol E D, Dimone V L and El-Asser M S 2001 XPS and FTIR surface characterization of TiO_2 particles used in polymer encapsulation *Langmuir* **17** 2664–9

[27] Wagner C D *et al* 1979 *Handbook of X-Ray Photoelectron Spectroscopy: A Reference Book of Standard Data for use in X-Ray Photoelectron Spectroscopy* (Eden Prairie, MN: Perkin-Elmer Corp.)